Distribution Locational Marginal Pricing Based Equilibrium Optimization Strategy for Data Center Park with Spatial-temporal Demand-side Resources

Zhihao Yang, *Graduate Student Member*, *IEEE*, Anupam Trivedi, *Member*, *IEEE*, Ming Ni, *Senior Member*, *IEEE*, Haoming Liu, *Senior Member*, *IEEE*, and Dipti Srinivasan, *Fellow*, *IEEE*

***Abstract*—This paper proposes a distribution locational marginal pricing (DLMP) based bi-level Stackelberg game framework between the internet service company (ISC) and distribution system operator (DSO) in the data center park. To minimize electricity costs, the ISC at the upper level dispatches the interactive workloads (IWs) across different data center buildings spatially and schedules the battery energy storage system temporally in response to DLMP. Photovoltaic generation and static var generation provide extra active and reactive power. At the lower level, DSO calculates the DLMP by minimizing the total electricity cost under the two-part tariff policy and ensures that the distribution network is uncongested and bus voltage is within the limit. The equilibrium solution is obtained by converting the bi-level optimization into a single-level mixed-integer second-order cone programming optimization using the strong duality theorem and the binary expansion method. Case studies verify that the proposed method benefits both the DSO and ISC while preserving the privacy of the ISC. By taking into account the uncertainties in IWs and photovoltaic generation, the flexibility of distribution networks is enhanced, which further facilitates the accommodation of more demand-side resources.**

***Index Terms*—Bi-level optimization, congestion management, data center, demand response, distribution locational marginal pricing (DLMP), robust optimization.**

NOMENCLATURE

A. Indices and Sets

π^{P}	Strategy set of distribution system operator (DSO)
Θ_j	Set of receiving buses of branch lines with the same sending bus j
B	Set of all branch lines in distribution network
D	Set of locations of data centers ($D \subseteq N$)
h	Index of binary extension method slice
i, j, k	Indices of buses in distribution network
N	Set of all buses in distribution network
P^{net}	Strategy set of player internet service company (ISC)
t	Index of time slots
T	Set of time slots

B. Variables

$\pi^{\mathrm{P}}_{j,t}$	Dual variable of nodal active power balance constraint as well as distribution locational marginal pricing
$\pi^{\mathrm{Q}}_{j,t}$	Dual variable of nodal reactive power balance constraint
$\pi^{\mathrm{v}}_{j,t}$	Dual variable of voltage drop constraint of each branch
$\lambda^{\mathrm{P}}_{ij,t}, \lambda^{\mathrm{Q}}_{ij,t}, \lambda^{\mathrm{lv1}}_{ij,t}, \lambda^{\mathrm{lv2}}_{ij,t}$	Dual variables of second-order cone programming relaxation constraint
$\delta^{\varphi-}_t, \delta^{\varphi+}_t$	Dual variables of lower/upper grid power factor limitation constraints
$\delta^{\mathrm{v}-}_{j,t}, \delta^{\mathrm{v}+}_{j,t}$	Dual variables of bus voltage magnitudes constraints
$\delta^{\mathrm{l}-}_{j,t}, \delta^{\mathrm{l}+}_{j,t}$	Dual variables of branch current magnitudes constraints
δ^{md}_t	Dual variable of the maximum power demand constraint
$A_{j,t}$	Number of active servers in data center building (DCB)
$E^{\mathrm{B}}_{j,t}$	Stored electric energy of bettary energy storage system (BESS)
F^{UL}	Payoff function of upper level
F^{LL}	Payoff function of lower level
$l_{ij,t}$	Squared current magnitude of branch (i, j)

Manuscript received: July 26, 2022; revised: November 11, 2022; accepted: January 30, 2023. Date of CrossCheck: January 30, 2023. Date of online publication: March 16, 2023.

This work was supported in part by the 2021 Graduate Research and Innovation Program of Jiangsu, China (No. KYCX21_0473) and the China Scholarship Council (CSC) Program (No. 202106710110).

Z. Yang, M. Ni (corresponding author), and H. Liu are with the College of Energy and Electrical Engineering, Hohai University, Nanjing 211100, China (e-mail: yang_zhihao@hhu.edu.cn; mingni2002@hotmail.com; liuhaom@hhu.edu.cn).

A. Trivedi and D. Srinivasan are with the Department of Electrical & Computer Engineering, National University of Singapore, Singapore (e-mail: eleatr@nus.edu.sg; dipti@nus.edu.sg).

DOI: 10.35833/MPCE.2022.000450

$L_{j,t}^{\mathrm{DC}}$ Total arriving workloads in DCB

m_t^{DC}, n_t^{DC}, $m_{j,t}^{\mathrm{PV}}$, $n_{j,t}^{\mathrm{PV}}$ Dual variables

$P_{j,t}^{\mathrm{DC}}$ Total active power load of DCB

$P_{j,t}^{\mathrm{PV}}$, $Q_{j,t}^{\mathrm{PV}}$ Active and reactive power outputs of photovoltaic (PV)

$P_{j,t}^{\mathrm{BC}}$, $P_{j,t}^{\mathrm{BD}}$ Charging and discharging active power of BESS

$P_{j,t}^{\mathrm{net}}$, $Q_{j,t}^{\mathrm{net}}$ Active and reactive net electric power

P^{md} The maximum demand for electric power

$P_{ij,t}$, $Q_{ij,t}$ Active and reactive power on branch (i, j)

P_t^{grid}, Q_t^{grid} Provided active and reactive power of data center park (DCP) by independent system operator (ISO)

$Q_{j,t}^{\mathrm{SVG}}$ Reactive power output of static var generation (SVG)

$u_{j,t}^{\mathrm{BC}}$, $u_{j,t}^{\mathrm{BD}}$ Binary variables indicating charging and discharging states of BESS

$v_{j,t}$ Squared voltage magnitude

y_t^{DC}, $y_{j,t}^{\mathrm{PV}}$ Auxiliary variables

C. Parameters

Γ_t^{DC}, $\Gamma_{j,t}^{\mathrm{PV}}$ Nonnegative control parameters between 0 and 1

Δt Time slot

η_j^{BC}, η_j^{BD} Charging and discharging efficiencies of BESS

ξ^{front}, ξ^{PV} Uncertainties of parameters $\tilde{L}_t^{\mathrm{front}}$ and $\tilde{T}_t^{\mathrm{PV}}$

ρ Number of days to settle the maximum demand price

φ^{grid} Power factor of DCP

$A_{j,\max}$ The maximum number of servers

c_t^{grid} Purchased electricity price of DSO

c^{md} The maximum demand price of DSO

C_j^{PUE} Designed power usage efficiency (PUE) of a DCB

C^{DT} The maximum delay time

E_j^{RB} Rated energy of BESS

H A non-negative integer

$I_{ij,\max}$ Upper bound of current magnitude of branch (i, j)

L_j^{rate} Service rate of a server

L_t^{front}, $\tilde{L}_t^{\mathrm{front}}$ Predicted and uncertain workloads in front-end server

M_j Big positive constant

P_j^{idle}, P_j^{peak} Idle and peak active power of a server

$P_{j,t}^{\mathrm{BL}}$, $Q_{j,t}^{\mathrm{BL}}$ Basic active and reactive power loads

$P_{j,\max}^{\mathrm{B}}$ The maximum active charging or discharging power of BESS

$P_{j,\max}^{\mathrm{net}}$ The maximum net electric power

$Q_{j,\max}^{\mathrm{SVG}}$ Reactive power capacity of SVG

r_{ij}, x_{ij} Resistance and reactance of branch (i, j)

$S_{j,\max}^{\mathrm{PV}}$ Apparent power capacity of PV

$SOC_{j,\min}$, $SOC_{j,\max}$ The minimum and maximum states-of-charge (SOCs) of BESS

T_t^{PV}, $\tilde{T}_t^{\mathrm{PV}}$ Day-ahead predicted and uncertain active power output curves of PV

$V_{j,\min}$, $V_{j,\max}$ Lower and upper voltage bounds

I. Introduction

CLOUD computing is gaining momentum, driven by the development of social networks, big data, and the Internet of Things. To effectively process these massive workloads and provide reliable computing services, major internet service companies (ISCs) have built extensive data centers. With the expansion of data centers, their energy consumption has grown rapidly, most of which are used for processing workloads and corresponding cooling systems. On a global scale, the annual electric power consumption of data centers reached around 3% in 2016 [1], and the rates have increased steadily in the recent few years [2]. To make full use of the infrastructure resources, several data center buildings (DCBs) are usually centrally placed in an industrial park. For example, Amazon has built many data centers all over the world, most of which are placed in the same park with multiple DCBs [3]. A leading communication company StarHub also has seven data centers across Singapore, some of which are built in the same park [4]. These DCBs are powered by the park distribution network and distributed in different buses. In some countries, these industrial parks with multiple DCBs are named data center parks (DCPs) [5]. For some newly built DCPs, the line capacities of the distribution network are usually matched with all DCBs at full loads. However, for some existing DCPs, the high penetration of electrical loads (ELs) of DCBs may cause network congestion and voltage off-limit [6], which endangers the systems' security.

The traditional methods to block out network congestion are expanding the power capacity or network reconfiguration [7], but the costs are relatively high. To avoid changing the distribution network structure, the pricing control method is a novel method to incentivize demand-side resources, e. g., photovoltaic (PV) [8], battery energy storage systems (BESSs) [9], thermal loads [6], and electric vehicle charging stations [10], to proactively respond to the grid demand. Derived from the locational marginal pricing method in the power transmission market, the distribution locational marginal pricing (DLMP) method is developed in recent years as a pricing method to address network congestion and voltage issues in the distribution networks [8]-[10]. The DLMPs, including the marginal electric power price, marginal loss price, marginal voltage support price, and marginal congestion price, can promote end-users to manage the demand-side resources to reduce electricity costs. However, to make the problem easy to solve, many studies use direct current optimal power flow (DCOPF) and power transfer distribution factor to calculate DLMP [11], [12], which carries great errors because line reactance cannot be ignored in the distribution network.

The thermal loads, BESSs, and electric vehicle charging

stations are temporal demand-side resources, which can be dispatched in different time slots for congestion management. Different from temporal demand-side resources, the arriving workloads at the front-end server can be dispatched both temporally and spatially through the data network. According to the processing deadlines, the arriving workloads mainly include the delay-tolerant batch workloads (BWs) and delay-sensitive interactive workloads (IWs) [13]. Delay-torrent BWs in a DCB can be scheduled to any time slot to process within the deadline temporally, while delay-sensitive IWs can be dispatched to any DCB in the DCP within a time slot spatially. To this end, the net power of DCBs is scheduled to change the power flow of the distribution network thus supporting voltages and alleviating congestion issues. In addition, to improve the demand response potential of each DCB, auxiliary energy systems such as PV, static var generator (SVG), and BESS can be utilized.

In reality, data centers had participated in demand response in history. For example, on July 22, 2011, hundreds of data centers cut power demands for emergency demand response and helped avoid a wide-area blackout throughout North America [14]. Distribution network congestions and voltage issues typically occur in developed regions with heavy electricity loads, so some countries such as China have channeled more BWs from developed regions to less developed regions with more renewable energies [15]. As a result, the remaining IWs such as online trading and web browsing workloads, make up a significant portion of the demand-side resources in developed regions. Despite their flexibility, most existing studies only focus on minimizing energy costs for data centers, neglecting their potential contributions to supporting grid voltages and managing congestion [16], which would adversely affect power system security [17].

In the electricity market, the distribution networks for general industrial and commercial users are usually managed by the distribution system operators (DSOs), which are powered by the electricity utilities, e.g., independent system operators (ISOs). In terms of the DSO, the most effective method is scheduling all the available demand-side resources in a centralized manner. However, it is unrealistic for the DSO to gain access and control of all devices in the distribution network, particularly considering users' data privacy. To address this challenge, researchers have explored the use of the non-cooperative Stackelberg game theory, which models interactions between energy suppliers and consumers as leaders and followers [18]. This can protect users' privacy by requiring less information exchange such as device-specific information [19]. In [20], an equilibrium model involving a DSO, a supplying utility, prosumers, and conventional consumers is solved by the strong duality theorem. Hence, the optimization of follower DSO in the lower level should be either linear or convex such as with DistFlow. However, linearized DistFlow models with simplified power flow assumptions assume a fixed bus voltage of 1.0 p.u., which may not provide an accurate outer approximation of the original DistFlow model. This can result in the loss of feasible solutions or generate additional infeasible regions [21].

These studies seldom consider security issues such as network congestion and voltage issues in distribution networks. In [22], the Stackelberg game concept is employed to develop an incentive-based mechanism to involve flexible resources in the congestion management of the distribution network. However, only temporal flexible resources are considered in this paper. Motivating all temporal demand-side resources to operate in the same time slot may still result in distribution network congestion and voltage issues. Therefore, the spatial demand response is considered to further cope with the distribution network security issues.

Multiple uncertainties such as those in renewable generation and workloads can lead to uncontrollable distribution network congestion and other security issues that increase system risk and operation costs. It is crucial to incorporate such uncertainties into operation models to enhance the applicability of the proposed method in motivating DCBs to support grid security. Stochastic optimization (SO) [23], [24], robust optimization (RO) [25], [26], and distributionally robust optimization (DRO) [27], [28] are three widely used techniques for optimization under uncertainties. Since both SO and DRO rely on a large number of historical data, which may be difficult to obtain for interactive workloads, this paper adopts an RO method. Further, the RO problem is usually solved by Benders decomposition and column-and-constraint generation algorithm, which is rather complicated. Therefore, this paper takes an equivalent linear formulation of RO derived from [29] to tackle uncertainties in workloads and PV generation.

Compared with previous works, this paper proposes a DLMP-based equilibrium optimization strategy for DCP with spatial-temporal demand-side resources. The contributions of this paper are as follows.

1) A bi-level Stackelberg game framework is proposed to motivate multiple DCBs with demand-side resources to support the grid security, where the ISC with multiple DCBs is seen as a leader and DSO is seen as a follower.

2) Both the temporal and spatial demand-side resources of multiple DCBs are considered to be scheduled in the game strategy. The uncertainties in arriving workload and PV generations are modeled into RO format to verify the applicability of the proposed strategy in motivating DCBs to support grid security.

3) The radial distribution network is modeled by Disflow equations with the second-order cone programming (SOCP) formulation. To solve the bi-level operation problem, the strong duality equation of the SOCP problem is derived. The bilinear terms are addressed by the binary expansion method, thus converting the bi-level operation problem to a single-level mixed-integer second-order cone programming (MISOCP) problem, which can be solved by commercial solvers.

The rest of this paper is organized as follows. Section II presents the problem formulation, including the framework of DLMP-based equilibrium optimization strategy and the upper-level and lower-level dispatching models. Section III presents the model reformulation and solution method. Section IV presents the case studies on a modified IEEE 33-bus system. Conclusions are drawn in Section V.

II. Problem Formulation

A. Framework of DLMP-based Equilibrium Optimization Strategy

The basic structure of the problem in this paper includes three stakeholders: ISC, DSO, and ISO, as shown in Fig. 1. The participants in the Stackelberg game in DCP are the ISC and DSO. In this game, the ISC with multiple DCBs at different buses of the distribution network serves as the leader, while the DSO is the follower. The leader at the upper level optimizes the operation of demand-side resources, e.g., IWs, BESS, PV, SVG, to minimize the total electricity cost and send the net electric power demand to the DSO. Based on the net power at all buses and time slots, the DSO optimizes the security-constrained power flow of the distribution network and provides DLMPs to each consumer. In addition to ensuring grid security, minimizing the total electricity cost is also a concern for DSO. The DSO is assumed to be a price taker receiving the industrial two-part tariff (TPT) from ISO and providing the electric power demands to ISO [30]. Moreover, another two assumptions are summarized as follows.

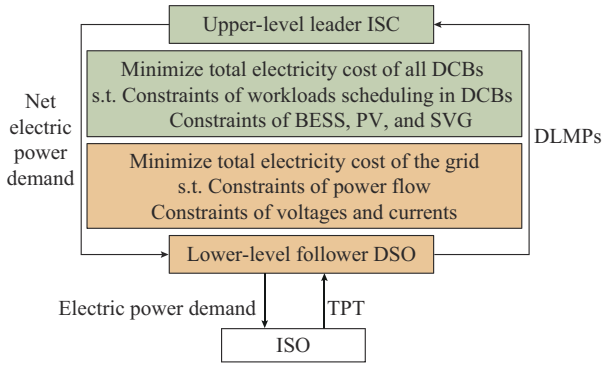

Fig. 1. Operation framework for ISC, DSO, and ISO.

1) Only DCBs are seen as the flexible loads in the distribution network of DCP. Other loads are seen to be fixed, and there are no distributed generations except PV generation in DCBs.

2) The coupling of multiple energy systems, e.g., electric power and natural gas, is neglected in the DCP.

To this end, the bi-level Stackelberg game model is formulated as:

$$\Omega = \left\{ \mathrm{ISC} \bigcup \mathrm{DSO}, P^{\mathrm{net}}, \pi^{\mathrm{P}}, F^{\mathrm{UL}}, F^{\mathrm{LL}} \right\} \tag{1}$$

where $P^{\mathrm{net}} = \left\{ P_{j,t}^{\mathrm{net}} \middle| j \in D, t \in T \right\}$; and $\pi^{\mathrm{P}} = \left\{ \pi_{j,t}^{\mathrm{P}} \middle| j \in D, t \in T \right\}$. Let $(\cdot)^*$ be the optimal strategies of each player, the equilibrium solution can be solved by:

$$\begin{cases} \left(P^{\mathrm{net}}\right)^* = \arg\min F^{\mathrm{UL}} \left\{ P^{\mathrm{net}}, \left(\pi^{\mathrm{P}}\right)^* \right\} \\ \text{s.t. } \left(\pi^{\mathrm{P}}\right)^* = \arg\min F^{\mathrm{LL}} \left\{ \left(P^{\mathrm{net}}\right)^*, \pi^{\mathrm{P}} \right\} \end{cases} \tag{2}$$

Remark 1: this paper assumes that multiple DCBs are managed by a single ISC. Therefore, the proposed bilevel problem is indeed a one-leader and one-follower Stackelberg game, where the equilibrium solution remains the same regardless of who serves as the leader or follower. Additionally, since the optimization of multiple DCBs with integer variables is non-convex, the ISC is set as the leader while the DSO is the follower for computational tractability.

B. Upper-level Dispatching Models

As the leader at the upper level, ISC manages several DCBs. The electric power load (EL) of these DCBs consists of IT energy consumption, e.g., servers, memory, communication, and storage devices, as well as other ancillary energy consumption, e.g., air conditioning, lighting. Power usage efficiency (PUE) is generally used to illustrate the relationship between IT energy consumption and ancillary energy consumption, which is defined as the ratio of total energy consumption to IT energy consumption [16]. In addition, to satisfy the reactive power loads of DCBs, the SVG and reactive capacity of PV are considered at the upper level. BESS also provides the temporal demand response potential of each DCB. As a rational game player, ISC would pursue the minimization of electric power costs. To this end, the upper-level model is formulated as:

$$\min F^{\mathrm{UL}} = \sum_{t \in T} \sum_{j \in D} \pi_{j,t}^{\mathrm{P}} P_{j,t}^{\mathrm{net}} \Delta t \tag{3a}$$

s.t.

$$P_{j,t}^{\mathrm{DC}} = \left[P_j^{\mathrm{idle}} + \left(C_j^{\mathrm{PUE}} - 1 \right) P_j^{\mathrm{peak}} \right] A_{j,t} + \frac{P_j^{\mathrm{peak}} - P_j^{\mathrm{idle}}}{L_j^{\mathrm{rate}}} L_{j,t}^{\mathrm{DC}} \quad \forall j \in D, \forall t \in T \tag{3b}$$

$$0 \le A_{j,t} \le A_{j,\max} \quad \forall j \in D, \forall t \in T \tag{3c}$$

$$\frac{1}{L_j^{\mathrm{rate}} A_{j,t} - L_{j,t}^{\mathrm{DC}}} \le C^{\mathrm{DT}} \quad \forall j \in D, \forall t \in T \tag{3d}$$

$$L_{j,t}^{\mathrm{DC}} \ge 0 \quad \forall j \in D, \forall t \in T \tag{3e}$$

$$\sum_{j \in D} L_{j,t}^{\mathrm{DC}} \ge \tilde{L}_t^{\mathrm{front}} \quad \forall t \in T \tag{3f}$$

$$0 \le P_{j,t}^{\mathrm{PV}} \le S_{j,\max}^{\mathrm{PV}} \tilde{T}_t^{\mathrm{PV}} \quad \forall j \in D, \forall t \in T \tag{3g}$$

$$\left| Q_{j,t}^{\mathrm{PV}} \right| \le S_{j,\max}^{\mathrm{PV}} \sqrt{1 - \left(T_t^{\mathrm{PV}} \right)^2} \quad \forall j \in D, \forall t \in T \tag{3h}$$

$$\left| Q_{j,t}^{\mathrm{SVG}} \right| \le Q_{j,\max}^{\mathrm{SVG}} \quad \forall j \in D, \forall t \in T \tag{3i}$$

$$E_{j,t}^{\mathrm{B}} = E_{j,t-1}^{\mathrm{B}} + \left(\eta_j^{\mathrm{BC}} P_{j,t}^{\mathrm{BC}} - \frac{P_{j,t}^{\mathrm{BD}}}{\eta_j^{\mathrm{BD}}} \right) \Delta t \quad \forall j \in D, \forall t \in T \setminus \{1\} \tag{3j}$$

$$E_{j,1}^{\mathrm{B}} = SOC_{j,1} E_j^{\mathrm{RB}} \quad \forall j \in D \tag{3k}$$

$$E_{j,1}^{\mathrm{B}} = E_{j,|T|}^{\mathrm{B}} \quad \forall j \in D \tag{3l}$$

$$SOC_{j,\min} E_j^{\mathrm{RB}} \le E_{j,t}^{\mathrm{B}} \le SOC_{j,\max} E_j^{\mathrm{RB}} \quad \forall j \in D, \forall t \in T \tag{3m}$$

$$0 \le \eta_j^{\mathrm{BC}} P_{j,t}^{\mathrm{BC}} \le P_{j,\max}^{\mathrm{B}} u_{j,t}^{\mathrm{BC}} \quad \forall j \in D, \forall t \in T \tag{3n}$$

$$0 \le \frac{P_{j,t}^{\mathrm{BD}}}{\eta_j^{\mathrm{BD}}} \le P_{j,\max}^{\mathrm{B}} u_{j,t}^{\mathrm{BD}} \quad \forall j \in D, \forall t \in T \tag{3o}$$

$$u_{j,t}^{\mathrm{BC}} + u_{j,t}^{\mathrm{BD}} \le 1 \quad \forall j \in D, \forall t \in T \tag{3p}$$

$$0 \le P_{j,t}^{\mathrm{net}} \le P_{j,\max}^{\mathrm{net}} \quad \forall j \in D, \forall t \in T \tag{3q}$$

$$P_{j,t}^{\mathrm{net}} + P_{j,t}^{\mathrm{PV}} + P_{j,t}^{\mathrm{BD}} = P_{j,t}^{\mathrm{BC}} + P_{j,t}^{\mathrm{DC}} + P_{j,t}^{\mathrm{BL}} \quad \forall j \in D, \forall t \in T \tag{3r}$$

$$Q_{j,t}^{\text{net}}+Q_{j,t}^{\text{SVG}}+Q_{j,t}^{\text{PV}}=Q_{j,t}^{\text{BL}}\quad \forall j\in D,\forall t\in T \tag{3s}$$

Equation (3a) is the objective function of the upper level, where $\pi_{j,t}^{\text{P}}$ is derived by the dual variable of the nodal active power balance constraint in the lower-level problem [8]. Constraint (3b) denotes the EL consumptions of DCBs on the bus j, which is determined by the number of active servers $A_{j,t}$ and arriving workload $L_{j,t}^{\text{DC}}$. Constraint (3c) limits the total number of on-service active servers. Constraint (3d) denotes the quality-of-service (QoS) requirement, in which waiting time is mainly considered based on the M/M/1 theory [31]. Constraints (3e) and (3f) indicate that the arriving IWs at the front-end server should be allocated to all DCBs without omission. Constraints (3g) and (3h) represent the active and reactive output power of PV generations, which take into account the minor differences between the natural conditions of DCBs within the same DCP. Each PV generation follows the same output trace but may vary in capacity. Constraint (3i) limits the output reactive power of SVG [30]. Constraints (3j) - (3p) are the BESS model [20]. Constraint (3q) determines the interactive net power between each DCB and the distribution network. Constraints (3r) and (3s) describe the active and reactive power balance with all demand-side resources.

If the uncertainties of PV generations and arriving IWs in the front-end servers are not considered, then $\tilde{L}_t^{\text{front}}=L_t^{\text{front}}$, $\tilde{T}_t^{\text{PV}}=T_t^{\text{PV}}$. However, their uncertainties would affect the decision-making of ISC. The detailed robust models are provided in Appendix A.

C. Lower-level Dispatching Models

As the follower in the bi-level framework, DSO receives the net power from the upper-level model and optimizes the power flow to ensure the economic and secure energy supply under the TPT policy. It is assumed that the cost of the maximum demand in a settlement cycle such as a month is decided by a typical day. The distribution network is typically considered a radial network to be modeled by DistFlow [21] and converted to a convex problem with SOCP [30]. To this end, the lower-level model is:

$$\min F^{\text{LL}}=\sum_{t\in T}c_t^{\text{grid}}P_t^{\text{grid}}\Delta t+\frac{1}{\rho}c^{\text{md}}P^{\text{md}} \tag{4a}$$

s.t.

$$P_{ij,t}=r_{ij}l_{ij,t}+\sum_{k\in\Theta_j}P_{jk,t}+P_{j,t}^{\text{net}}\quad \forall j\in D,\forall t\in T\quad \left(\pi_{j,t}^{\text{P}}\right) \tag{4b}$$

$$P_{ij,t}=r_{ij}l_{ij,t}+\sum_{k\in\Theta_j}P_{jk,t}+P_{j,t}^{\text{BL}}\quad \forall j\in N\backslash\{1\}\backslash D,\forall t\in T\quad \left(\pi_{j,t}^{\text{P}}\right) \tag{4c}$$

$$P_t^{\text{grid}}=\sum_{k\in\Theta_1}P_{1k,t}\quad \forall t\in T\quad \left(\pi_{1,t}^{\text{P}}\right) \tag{4d}$$

$$Q_{ij,t}=x_{ij}l_{ij,t}+\sum_{k\in\Theta_j}Q_{jk,t}+Q_{j,t}^{\text{BL}}\quad \forall j\in N\backslash\{1\},\forall t\in T\quad \left(\pi_{j,t}^{\text{Q}}\right) \tag{4e}$$

$$Q_t^{\text{grid}}=\sum_{k\in\Theta_1}Q_{1k,t}\quad \forall t\in T\quad \left(\pi_{1,t}^{\text{Q}}\right) \tag{4f}$$

$$v_{j,t}=v_{i,t}-2\left(r_{ij}P_{ij,t}+x_{ij}Q_{ij,t}\right)+\left(r_{ij}^2+x_{ij}^2\right)l_{ij,t}\quad \forall\left(i,j\right)\in B,\forall t\in T\quad \left(\pi_{ij,t}^{\text{v}}\right) \tag{4g}$$

$$\left\|\begin{matrix}2P_{ij,t}\\2Q_{ij,t}\\l_{ij,t}-v_{i,t}\end{matrix}\right\|\le l_{ij,t}+v_{i,t}\quad \forall\left(i,j\right)\in B,\forall t\in T\quad \left(\begin{bmatrix}\lambda_{ij,t}^{\text{P}}\\\lambda_{ij,t}^{\text{Q}}\\\lambda_{ij,t}^{\text{lv1}}\end{bmatrix},\lambda_{ij,t}^{\text{lv2}}\right) \tag{4h}$$

$$-P_t^{\text{grid}}\tan\varphi^{\text{grid}}\le Q_t^{\text{grid}}\le P_t^{\text{grid}}\tan\varphi^{\text{grid}}\quad \forall t\in T\quad \left(\delta_t^{\varphi-},\delta_t^{\varphi+}\right) \tag{4i}$$

$$V_{j,\min}^2\le v_{j,t}\le V_{j,\max}^2\quad \forall j\in N,\forall t\in T\quad \left(\delta_{j,t}^{\text{v}-},\delta_{j,t}^{\text{v}+}\right) \tag{4j}$$

$$0\le l_{ij,t}\le I_{ij,\max}^2\quad \forall\left(i,j\right)\in B,\forall t\in T\quad \left(\delta_{ij,t}^{\text{l}-},\delta_{ij,t}^{\text{l}+}\right) \tag{4k}$$

$$P_t^{\text{grid}}\le P^{\text{md}}\quad \forall t\in T\quad \left(\delta_t^{\text{md}}\right) \tag{4l}$$

Note that the variables in the brackets are dual variables of constraints. The objective function (4a) aims at minimizing the total electricity cost of the DCP. Constraints (4b)-(4f) state the nodal active and reactive power balance. Constraint (4g) formulates the voltage drop of each branch. Constraint (4h) indicates SOCP relaxation. Constraint (4i) represents the limitation of grid power factors by ISO. Constraints (4j) and (4k) limit the magnitudes of bus voltages and branch currents, respectively. Constraint (4) indicates the maximum demand for grid power.

III. Model Reformulation and Solution Method

Based on the framework proposed in Section II, DLMPs derived from the dual multipliers of the lower-level distribution system operation model should be provided for consumers including all DCBs. According to the dual theorem of the convex SOCP problem [32], the dual form of the lower-level model in (4) is reformulated as:

$$\begin{aligned}\max\ &\sum_{t\in T}\sum_{j\in D}\pi_{j,t}^{\text{P}}P_{j,t}^{\text{net}}+\sum_{t\in T}\sum_{j\in N\backslash\{1\}\backslash D}\pi_{j,t}^{\text{P}}P_{j,t}^{\text{BL}}+\sum_{t\in T}\sum_{j\in N\backslash\{1\}}\pi_{j,t}^{\text{Q}}Q_{j,t}^{\text{BL}}+\\&\sum_{t\in T}\sum_{j\in N}\left(V_{j,\min}^2\delta_{j,t}^{\text{v}-}-V_{j,\max}^2\delta_{j,t}^{\text{v}+}\right)-\sum_{t\in T}\sum_{(i,j)\in B}I_{ij,\max}^2\delta_{ij,t}^{\text{l}+}\end{aligned} \tag{5a}$$

s.t.

$$-\pi_{i,t}^{\text{P}}+\pi_{j,t}^{\text{P}}+2r_{ij}\pi_{ij,t}^{\text{v}}+2\lambda_{ij,t}^{\text{P}}=0\quad \forall\left(i,j\right)\in B,\forall t\in T\quad \left(P_{ij,t}\right) \tag{5b}$$

$$-\pi_{i,t}^{\text{Q}}+\pi_{j,t}^{\text{Q}}+2x_{ij}\pi_{ij,t}^{\text{v}}+2\lambda_{ij,t}^{\text{Q}}=0\quad \forall\left(i,j\right)\in B,\forall t\in T\quad \left(Q_{ij,t}\right) \tag{5c}$$

$$\pi_{1,t}^{\text{P}}+\left(\delta_t^{\varphi-}+\delta_t^{\varphi+}\right)\tan\varphi^{\text{grid}}-\delta_t^{\text{md}}=c_t^{\text{grid}}\Delta t\quad \forall t\in T\quad \left(P_t^{\text{grid}}\right) \tag{5d}$$

$$\pi_{1,t}^{\text{Q}}+\delta_t^{\varphi-}-\delta_t^{\varphi+}=0\quad \forall t\in T\quad \left(Q_t^{\text{grid}}\right) \tag{5e}$$

$$\sum_{t\in T}\delta_t^{\text{md}}=\frac{1}{\rho}c^{\text{md}}\quad \left(P^{\text{md}}\right) \tag{5f}$$

$$-r_{ij}\pi_{j,t}^{\text{P}}-x_{ij}\pi_{j,t}^{\text{Q}}-\left(r_{ij}^2+x_{ij}^2\right)\pi_{ij,t}^{\text{v}}+\lambda_{ij,t}^{\text{lv1}}+\lambda_{ij,t}^{\text{lv2}}+\delta_{ij,t}^{\text{l}-}-\delta_{ij,t}^{\text{l}+}=0\quad \forall\left(i,j\right)\in B,\forall t\in T\quad \left(l_{ij,t}\right) \tag{5g}$$

$$-\sum_{k\in\Theta_1}\left(\pi_{1k,t}^{\text{v}}+\lambda_{1k,t}^{\text{lv1}}-\lambda_{1k,t}^{\text{lv2}}\right)+\delta_{1,t}^{\text{v}-}-\delta_{1,t}^{\text{v}+}=0\quad \forall t\in T\quad \left(v_{1,t}\right) \tag{5h}$$

$$\pi_{ij,t}^{\text{v}}-\sum_{k\in\Theta_j}\left(\pi_{jk,t}^{\text{v}}+\lambda_{jk,t}^{\text{lv1}}-\lambda_{jk,t}^{\text{lv2}}\right)+\delta_{j,t}^{\text{v}-}-\delta_{j,t}^{\text{v}+}=0\quad \forall j\in N/\{1\},\forall t\in T\quad \left(v_{j,t}\right) \tag{5i}$$

$$\left\| \begin{matrix} \lambda_{ij,t}^{\mathrm{P}} \\ \lambda_{ij,t}^{\mathrm{Q}} \\ \lambda_{ij,t}^{\mathrm{lv1}} \end{matrix} \right\|_2 \le \lambda_{ij,t}^{\mathrm{lv2}} \quad \forall (i,j) \in B, \forall t \in T \tag{5j}$$

$$\begin{cases} \delta_t^{\varphi-} \ge 0 \\ \delta_t^{\varphi+} \ge 0 \\ \delta_t^{\mathrm{md}} \ge 0 \end{cases} \quad \forall t \in T \tag{5k}$$

$$\begin{cases} \delta_{j,t}^{\mathrm{v}-} \ge 0 \\ \delta_{j,t}^{\mathrm{v}+} \ge 0 \end{cases} \quad \forall j \in N, \forall t \in T \tag{5l}$$

$$\begin{cases} \delta_{ij,t}^{\mathrm{l}-} \ge 0 \\ \delta_{ij,t}^{\mathrm{l}+} \ge 0 \end{cases} \quad \forall (i,j) \in B, \forall t \in T \tag{5m}$$

Equations (5b) - (5i) are dual constraints associated with the primal variables in the brackets. Constraint (5j) is the dual counterpart of the primal SOCP constraint (4h), which is also a SOCP constraint. Constraints (5k)-(5m) limit the values of dual multipliers.

Since the primal problem and the dual problem of the lower level are both convex, the strong duality equality holds:

$$(4a) = (5a) \tag{6}$$

Then, the bi-level problem (2) can be equivalently transformed into the following single-level problem:

$$\begin{cases} \min \sum_{t \in T} \sum_{j \in D} \pi_{j,t}^{\mathrm{P}} P_{j,t}^{\mathrm{net}} \Delta t \\ \text{s.t. Upper - level constraints: (3b) - (3s)} \\ \quad \text{Lower - level constraints: (4b) - (4l), (5b) - (5m), (6)} \end{cases} \tag{7}$$

Note that the above single-level problem has the bilinear terms $\pi_{j,t}^{\mathrm{P}} P_{j,t}^{\mathrm{net}}$, which cannot be solved directly by commercial solvers such as CPLEX and GUROBI. To deal with the bilinear terms, a binary expansion (BE) scheme is used to discretize one of the continuous variables and convert the non-linear problem into an MILP problem [33].

The basic idea of BE method in this paper is to approximate the continuous decision values $P_{j,t}^{\mathrm{net}}$ by a set of discrete values $\left\{ P_{j,t,h}^{\mathrm{net}} \middle| h = 0, 1, \ldots, \Xi \right\}$, where $\Xi = 2^H$ is a non-negative integer that decides the number of slices. As $P_{j,t}^{\mathrm{net}}$ satisfies the constraint (3q), the discrete approximation can be expressed as:

$$P_{j,t}^{\mathrm{net}} = P_{j,t}^{\mathrm{BL}} + \frac{P_{j,\max}^{\mathrm{net}} - P_{j,t}^{\mathrm{BL}}}{2^H} \sum_{h=0}^{H} 2^h u_{j,t,h}^{\mathrm{Pnet}} \quad \forall j \in D, \forall t \in T \tag{8}$$

where $u_{j,t,h}^{\mathrm{Pnet}}$ is a binary variable. Multiplying both sides of (8) by $\pi_{j,t}^{\mathrm{P}}$, and defining $z_{j,t,h}^{\mathrm{Pnet}} = u_{j,t,h}^{\mathrm{Pnet}} \pi_{j,t}^{\mathrm{P}}$, we can obtain:

$$\pi_{j,t}^{\mathrm{P}} P_{j,t}^{\mathrm{net}} = \pi_{j,t}^{\mathrm{P}} P_{j,t}^{\mathrm{BL}} + \frac{P_{j,\max}^{\mathrm{net}} - P_{j,t}^{\mathrm{BL}}}{2^H} \sum_{h=0}^{H} 2^h z_{j,t,h}^{\mathrm{Pnet}} \quad \forall j \in D, \forall t \in T \tag{9}$$

$$0 \le \pi_{j,t}^{\mathrm{P}} - z_{j,t,h}^{\mathrm{Pnet}} \le \left(1 - u_{j,t,h}^{\mathrm{Pnet}}\right) M_j \quad \forall j \in D, \forall t \in T \tag{10}$$

$$0 \le z_{j,t,h}^{\mathrm{Pnet}} \le u_{j,t,h}^{\mathrm{Pnet}} M_j \quad \forall j \in D, \forall t \in T \tag{11}$$

where M_j is large enough for constraint (10) and constraint (11) to be relaxed when $u_{j,t,h}^{\mathrm{Pnet}} = 0$ and $u_{j,t,h}^{\mathrm{Pnet}} = 1$, respectively, e.g., $M_j = P_{j,\max}^{\mathrm{net}}$. Then, (6) becomes:

$$\begin{aligned} &\sum_{t \in T} c_t^{\mathrm{grid}} P_t^{\mathrm{grid}} \Delta t + \frac{1}{\rho} c^{\mathrm{md}} P^{\mathrm{md}} = \\ &\sum_{t \in T} \sum_{j \in D} \left(\pi_{j,t}^{\mathrm{P}} P_{j,t}^{\mathrm{BL}} + \frac{P_{j,\max}^{\mathrm{net}} - P_{j,t}^{\mathrm{BL}}}{2^H} \sum_{h=0}^{H} 2^h z_{j,t,h}^{\mathrm{Pnet}} \right) + \\ &\sum_{t \in T} \sum_{j \in N \setminus \{1\} \setminus D} \pi_{j,t}^{\mathrm{P}} P_{j,t}^{\mathrm{BL}} + \sum_{t \in T} \sum_{j \in N \setminus \{1\}} \pi_{j,t}^{\mathrm{Q}} Q_{j,t}^{\mathrm{BL}} + \\ &\sum_{t \in T} \sum_{j \in N} \left(V_{j,\min}^2 \delta_{j,t}^{\mathrm{v}-} - V_{j,\max}^2 \delta_{j,t}^{\mathrm{v}+} \right) - \sum_{t \in T} \sum_{(i,j) \in B} I_{ij,\max}^2 \delta_{ij,t}^{\mathrm{l}+} \end{aligned} \tag{12}$$

Finally, the single-level problem (7) is approximately equivalent to the following MISOCP problem, which can be solved by commercial solvers.

$$\begin{cases} \min \sum_{t \in T} \sum_{j \in D} \left(\pi_{j,t}^{\mathrm{P}} P_{j,t}^{\mathrm{BL}} + \frac{P_{j,\max}^{\mathrm{net}} - P_{j,t}^{\mathrm{BL}}}{2^H} \sum_{h=0}^{H} 2^h z_{j,t,h}^{\mathrm{Pnet}} \right) \Delta t \\ \text{s.t. Upper - level constraints: (3b) - (3s)} \\ \quad \text{Lower - level constraints: (4b) - (4l), (5b) - (5m), (6), (8) - (12)} \end{cases} \tag{13}$$

IV. Case Studies and Result Analysis

This section uses a modified IEEE 33-bus radial distribution network with four DCBs located at buses 18, 22, 25, and 33 in four regions with different colors to illustrate the DCP power system, as shown in Fig. 2. In this test, each DCB contains EL, BESS, SVG, and PV. The front-end server of ISC is responsible for allocating the arriving IWs to the four DCBs. DSO manages the DCP distribution power system and purchases electric power from ISO. The code is implemented in MATLAB R2016a with the YALMIP platform on a desktop with an Intel Core i9 CPU clocked at 3.0 GHz and 64 GB RAM. The optimization model is solved using Gurobi 9.5 solver.

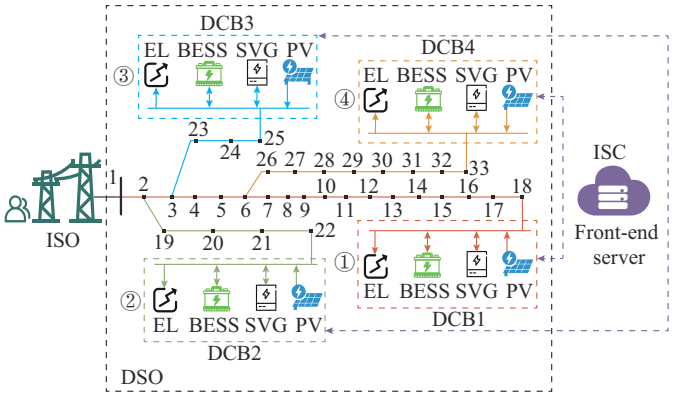

Fig. 2. Structure of DCP power system with four DCBs.

A. System Data and Case Description

To make the expression more concise, some indices of variables and constants are neglected in this subsection. The base voltage and base apparent power are considered to be 12.66 kV and 10 MVA, respectively. The power factor φ^{grid} is limited to 0.8. The voltage limits at each bus are 0.9 p.u. and 1.1 p.u., respectively [34]. The substation voltage is assumed to be 1.0 p.u.. The current limits in four regions are

set to be [595, 120, 120, 120]A. Figure 3 shows the daily basic EL curve without DCBs, the front-end IW curve, and the PV curve. The number of basic arriving IWs is set to be 1.5×10^4 requests per second. The electricity prices in Fig. 4 refer to the industrial TPT prices in Shanghai, China [35]. The charge as per the maximum demand is 34.02 CNY/kW each month. Detailed parameters are provided in Table I [36].

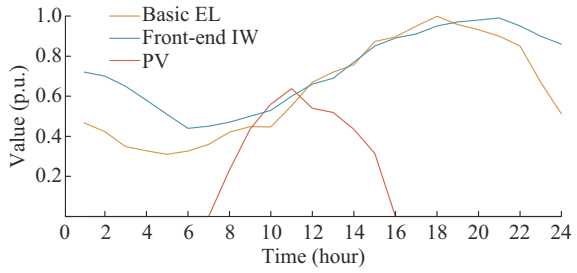

Fig. 3. Daily basic EL curve, front-end IW curve, and PV curve.

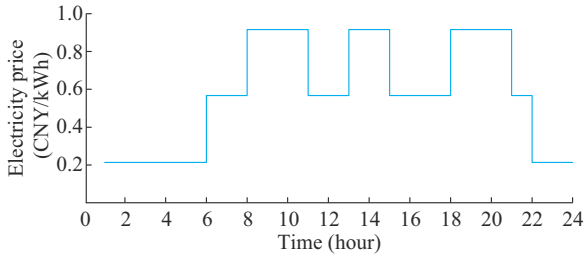

Fig. 4. Daily electricity prices.

TABLE I
PARAMETERS OF EL, BESS, SVG, AND PV

Component	Parameter	Value	Component	Parameter	Value
EL	A_{max}	[4000, 4000, 3000, 3000]	BESS	η^{BC}	[0.95, 0.95, 0.95, 0.95]
	L^{rate}	[4, 4, 4, 4] requests per second		η^{BD}	[0.95, 0.95, 0.95, 0.95]
	P^{idle}	[100, 100, 100, 100]W		SOC_{min}	[0.1, 0.1, 0.1, 0.1]
	P^{peak}	[200, 200, 200, 200]W		SOC_{max}	[0.9, 0.9, 0.9, 0.9]
	C^{PUE}	[1.35, 1.4, 1.4, 1.35]		SOC_1	[0.5, 0.5, 0.5, 0.5]
	C^{DT}	0.5 s		P^{B}_{max}	[100, 80, 80, 100]kW
	P^{net}_{max}	[1.2, 1.2, 1.2, 1.2]MW		E^{RB}	[250, 200, 200, 250]kWh
PV	S^{PV}_{max}	[150, 120, 120, 150]kVA	SVG	Q^{SVG}_{max}	[50, 50, 50, 50]kvar

In an electricity market where information is completely private, every entity has to make the strategy individually, which could adversely affect the profits of others. On the contrary, in a completely public electricity market, it needs to collect all entities' information in the centralized optimization, making it easy to be attacked when the information is leaked. To illustrate the advantages of the proposed equilibrium optimization in benefiting both DSO and ISC in terms of economy and privacy protection, three cases and their subcases are set for comparison, as summarized in Table II.

TABLE II
SUMMARY OF ALL CASES AND SUBCASES

Case	Subcase	Entity	Price	Demand-side resource
Case 1	Subcase 1.1	DSO	TPT	None
	Subcase 1.2	ISC	TPT	All
Case 2	Subcase 2.1	DSO	TPT	Without IW
	Subcase 2.2	DSO	TPT	All
	Subcase 2.3	ISC	TPT	All
Case 3	Subcase 3.1	Both	TPT	All
	Subcase 3.2	Both	DLMPs	All
	Subcase 3.3	Both	DLMPs	Without BESS
	Subcase 3.4	Both	DLMPs	Without IW

1) Case 1: Individual Optimization

Subcase 1.1: DSO optimizes the power flow without considering the net power of all DCBs.

Subcase 1.2: ISC optimizes all DCBs without considering the park distribution network power flow, then DSO takes the net power of all DCBs and optimizes the power flow.

2) Case 2: Centralized Optimization

Subcase 2.1: DSO optimizes the power flow considering demand-side resources except for IWs in DCBs.

Subcase 2.2: DSO optimizes the power flow considering all demand-side resources in DCBs.

Subcase 2.3: ISC optimizes all demand-side resources in DCBs considering the park distribution network power flow.

3) Case 3: Equilibrium Optimization

Subcase 3.1: ISC games with DSO using the proposed strategy by the electricity prices from ISO. All demand-side resources are considered.

Subcase 3.2: ISC games with DSO using the proposed strategy by DLMPs. All demand-side resources are considered.

Subcase 3.3: ISC games with DSO using the proposed strategy by DLMPs. BESS is not considered a flexible resource.

Subcase 3.4: ISC games with DSO using the proposed strategy by DLMPs. IWs are not considered flexible resources.

B. Impact of Demand-side Resources on Voltage and Power Flow

In Case 1, the ISC optimizes four DCBs based on electricity prices from ISO. As shown in Fig. 3, the basic EL and the total front-end IWs are relatively heavy at time slot 18, which might trigger voltage issues and power flow congestion. Taking time slot 18 as an example, the bus voltages are decreasing sharply away from the substation bus due to line losses, as shown in Fig. 5. Hence, the voltage is the lowest at bus 18 connected with DCB1. As shown in Fig. 6, most of the IWs are motivated to be dispatched to DCB1 and DCB4 because their PUE is smaller than that of DCB2 and DCB3. Hence, the currents of branches 25-29 in Fig. 7 are

over-limit I_{max} due to more EL at bus 18 and bus 33.

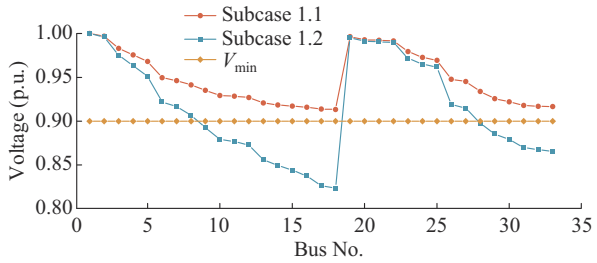

Fig. 5. Bus voltages in Case 1 at time slot 18.

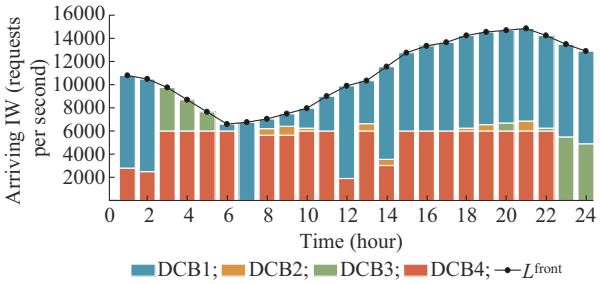

Fig. 6. Arriving IWs of DCBs in Case 1.

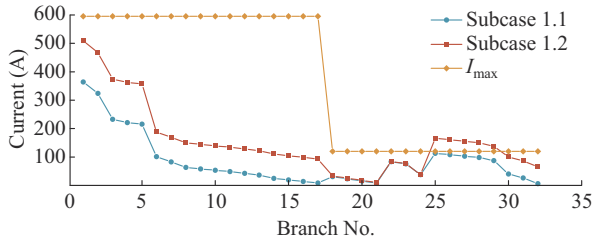

Fig. 7. Branch currents in Case 1 at time slot 18.

To ensure the distribution network security, i. e., without off-limit of voltages or congestion, the temporal and spatial demand responses are considered in Case 2 with centralized optimization. In terms of DSO, Subcase 2.1 mainly utilizes BESS as the temporal demand-side resource together with PV and SVG to support voltage and manage congestion, while Subcase 2.2 adds the IWs as flexible EL to provide spatial flexibility. In terms of ISC, Subcase 2.3 utilizes all the demand-side resources to minimize the electricity cost. Taking time slot 18 as an example, given the different objective functions compared with Subcases 2.1 and 2.2, ISC in Subcase 2.3 seeks less cost only if the bus voltages and branch currents are within the limit as shown in Fig. 8 and Fig. 9. It can be observed that the temporal demand response in Subcase 2.1 cannot effectively support voltages or manage congestion because BESS at each DCB is only the auxiliary equipment with a small capacity. By contrast, the EL caused by processing IWs in DCBs takes a large amount of net power, which significantly affects the power flow distribution. Under this condition, both strategies in Subcases 2.2 and 2.3 can satisfy the power flow constraints by dispatching IWs over four DCBs. However, the voltage at bus 18 and the current of branch 25 in Subcase 2.3 reach their limits, respectively, leading to voltage over-limit and power flow congestions in this area.

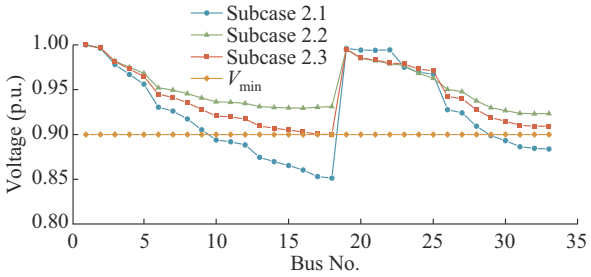

Fig. 8. Bus voltages in Case 2 at time slot 18.

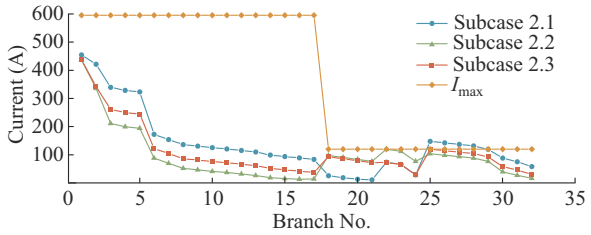

Fig. 9. Branch currents in Case 2 at time slot 18.

To protect the privacy of DCBs and alleviate the congestion, the proposed strategy is used in Case 3.

As shown in Fig. 10(a) and Fig. 11(a), the bus voltages and branch currents can both satisfy the constraints in Subcases 3.1 and 3.2. However, in Subcase 3.1, with the electricity prices from ISO directly taken in the ISC's strategy, the ISC does not have enough motivation to further implement demand response to support voltages and manage power flow congestion. In comparison, the DLMPs vary in different buses, as shown in Fig. 12. As all buses are power consumers, the DLMP at each bus is always larger than the electricity prices from ISO. When the bus voltages and branch currents are going to exceed the limits, the extra network loss costs, voltage support costs, and branch congestion costs would be added, and DLMPs increase. It incentivizes DCBs to further dispatch demand-side resources, e. g., BESSs and IWs. Hence, in Fig. 10(b), the gap between the voltages at bus 18 and the lower voltage limits in Subcase 3.2 is larger than that in Subcase 3.1. Similar results are revealed with the branch current, as shown in Fig. 11(b). Compared with centralized optimization in Subcase 2.2, the regulating effects of the proposed strategy on bus voltages and branch currents in Subcase 3.2 are slightly inferior due to the differences between DLMPs and electricity prices from ISO. However, the differences are marginal because the peak and valley periods of DLMPs and electricity prices from ISO are the same, as shown in Fig. 12. Nevertheless, DCBs' privacies are well protected since less private information is exchanged using the bi-level framework in Subcase 3.2.

C. Cost Analysis

The ISC with four DCBs needs to pay additional costs for network loss, voltage support, and branch congestion to DSO when being powered with the electricity prices from ISO in Case 1, Case 2, and Subcase 3.1. These additional costs can be shared equally with basic EL on other buses. In contrast, these additional costs are already added to the DLMPs in Subcase 3.2, i.e., the shared extra cost is zero.

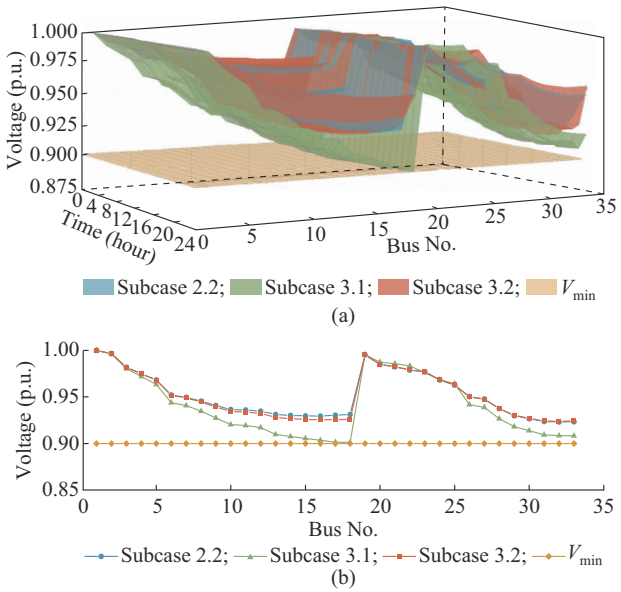

Fig. 10. Bus voltages in comparison with Subcases 2.2, 3.1, and 3.2. (a) Bus voltages in a day. (b) Bus voltages at time slot 18.

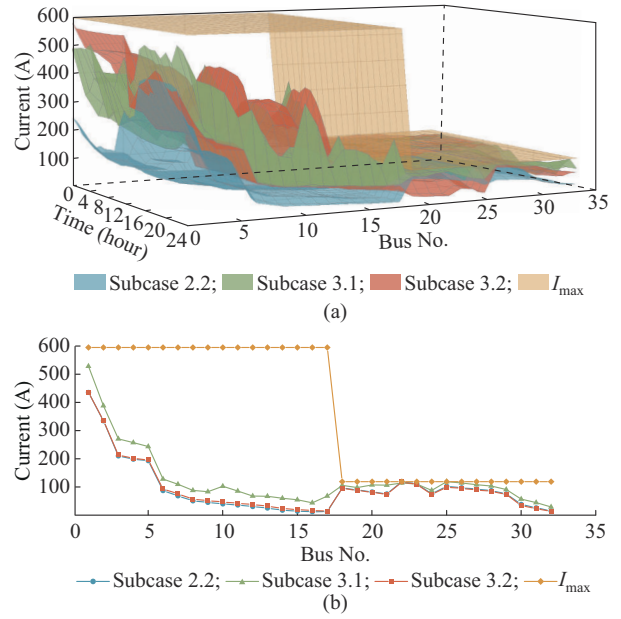

Fig. 11. Branch currents in comparison with Subcases 2.2, 3.1, and 3.2. (a) Branch currents in a day. (b) Branch currents at time slot 18.

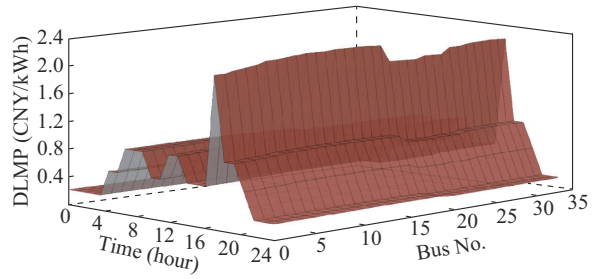

Fig. 12. DLMPs of active power in a day.

In terms of DSO, it is a precondition to keep all bus voltages within a safe level and make branches uncongested. The electric power costs of ISC and DSO with centralized optimization (Subcase 2.2) and equilibrium optimization (Subcases 3.1 and 3.2) are compared in Table III. The centralized optimization in Subcase 2.2 is the most economical strategy for DSO, of which the cost is 6.970% less than that in Subcase 3.1 and 0.372% less than that in Subcase 3.2. The cost difference between centralized optimization (Subcase 2.2) and DLMP-based equilibrium optimization (Subcase 3.2) is marginal. More importantly, due to the need for privacy protection for ISC, centralized optimization is almost impossible. Therefore, the proposed DLMP-based equilibrium optimization strategy provides a promising and cost-effective option.

TABLE III
COMPARISON OF ELECTRIC POWER COSTS WITH DIFFERENT STRATEGIES

Stake-holder	Cost type	Cost (10^4 CNY)		
		Subcase 2.2	Subcase 3.1	Subcase 3.2
DSO	Grid power cost	5.1047	5.4874	5.1223
	Capacity cost	0.5248	0.5639	0.5282
	Total cost	5.6295	6.0513	5.6505
	Extra cost	0.7606	1.2211	0.7711
ISC	Net power cost	2.0671	2.0284	2.3495
	Shared extra cost	0.2541	0.4021	0.0000
	Total cost	2.3212	2.4305	2.3495

In terms of ISC, the centralized optimization in Subcase 2.2 is also the most economic strategy, of which the cost is 4.497% less than that in Subcase 3.1 and 1.205% less than that in Subcase 3.2, respectively. Compared with the increase in energy costs in Subcase 3.2, privacy is much more important for ISC. Take time slot 18 as an example, where the DLMP at time slot 18 is relatively higher than in other time slots due to the peak of EL, as shown in Fig. 12. The net power of four DCBs in three subcases is compared in Fig. 13. The lower DLMPs at bus 22 and bus 25 motivate the ISC to dispatch more IWs to DCB2 and DCB3. In addition, the comparison of grid power of the distribution network in Subcases 2.2, 3.1, and 3.2 shown in Fig. 14 illustrate that the centralized optimization and the DLMP-based equilibrium optimization have similar dispatching results and power demand profiles due to the same objective function and constraints of DSO and ISC, thus indicating the effectiveness of the proposed DLMP-based equilibrium optimization strategy. However, compared with the increase in electricity costs in Subcase 3.2, privacy is much more important for ISC, making the proposed DLMP-based equilibrium optimization strategy the most suitable one. While in Subcase 3.1 with the same electricity prices for each bus, the ISC does not have enough economic incentive to further dispatch IWs to support grid security. Therefore, the grid power demand of the distribution system from the main grid in Subcase 3.1 is more than that in Subcase 2.2 and that in Subcase 3.2 as a whole.

In addition, although with the same TPT prices, the increased cost of ISC in Subcase 3.1 than that in Subcase 2.2 mainly results from the shared extra cost coming from the grid loss. However, the DLMP-based equilibrium game elim-

inates such drawbacks both for DSO and ISC. Compared with Subcase 3.1 without DLMPs, the proposed strategy in Subcase 3.2 saves 6.62% and 3.33% cost for DSO and ISC, respectively. In other words, the proposed strategy can incentivize more flexible users in the park to interact with the grid while preserving users' privacy, to enhance the cost-effectiveness and operational security of the distribution network.

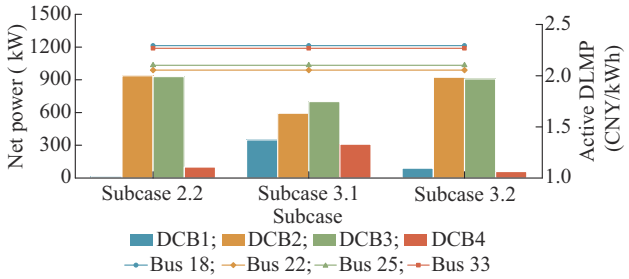

Fig. 13. Net power of four DCBs in three subcases at time slot 18.

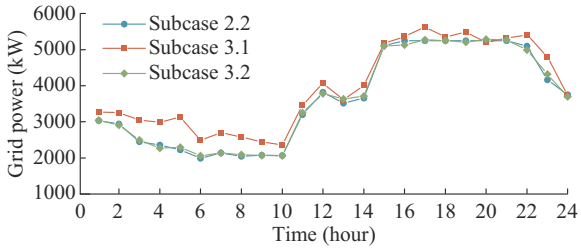

Fig. 14. Grid power of distribution network in three subcases.

In equilibrium optimization, the types of demand-side resources can also affect the economy of both DSO and ISC. It should be noted that the capacity of BESS is not very large in practice in these case studies with economic consideration. In this modified distribution network, random dispatching of IWs would render the optimization infeasible. The proportion of arriving IWs is taken as 20%, 30%, 30%, and 20% of the base loads in four DCBs in Subcase 3.4, respectively. The comparison of electric power costs with different resources in Subcases 3.2, 3.3, and 3.4 are provided in Table IV.

TABLE IV
COMPARISON OF ELECTRIC POWER COSTS WITH DIFFERENT RESOURCES

Stakeholder	Cost type	Cost (10^4 CNY)		
		Subcase 3.2	Subcase 3.3	Subcase 3.4
DSO	Grid power cost	5.1223	5.1415	5.2100
	Capacity cost	0.5282	0.5311	0.5599
	Total cost	5.6505	5.6726	5.7699
	Extra cost	0.7711	0.8079	0.8080
ISC	Net power cost	2.3495	2.3954	2.4921
	Shared extra cost	0.0000	0.0000	0.0000
	Total cost	2.3495	2.3954	2.4921

As shown in Table IV, the total cost of ISC in Subcase 3.4 is remarkably higher than that in Subcase 3.2 and that in Subcase 3.3, by 6.07% and 4.04%, respectively, due to the small capacity of BESS. It denotes that the dispatching IWs across different DCBs is much more economical in the equilibrium optimization considering DLMPs.

D. Uncertainty Analysis

The net power of DCBs is influenced by the arrival of IWs and PV generations, which are inherently uncertain in reality. According to the robust model in Appendix A, the parameters Γ_t^{DC} and $\Gamma_{j,t}^{\mathrm{PV}}$ control the robustness of the problem. For the sake of simplicity, it is assumed that Γ_t^{DC} and $\Gamma_{j,t}^{\mathrm{PV}}$ are taken as the same value Γ. In addition, the uncertain parameter ξ^{front} and parameter ξ^{PV} are seen as the same in this subsection. As shown in Table V, three uncertainty sets are listed with 5%, 8%, and 10% of the predicted values of the uncertainty variables [10]. Under any given value Γ, the increase of uncertainty also enlarges the cost of DSO and ISC except for $\Gamma=0$, where uncertainty makes no sense. Take $\Gamma=1$, $t=18$ as an example. As shown in Fig. 15(a) and (b), the DLMPs increase along with the uncertainty level. This is because with a higher level of uncertainty, the worst-case scenario results in an increase in the system's net power. With a smaller PUE indicator, more IWs with 10% uncertainty are dispatched to IDC4, thus slightly decreasing the number of IWs at IDC2 and IDC3. Thus, the differences in DLMPs vary slightly with an increase in uncertainty, primarily due to the impact of the net power of IDC2, IDC3, and IDC4.

TABLE V
COMPARISON OF ELECTRIC POWER COSTS OF DSO AND ISC UNDER DIFFERENT UNCERTAINTIES

Uncertainty (%)	Cost of DSO (10^4 CNY)			Cost of ISC (10^4 CNY)		
	$\Gamma=0$	$\Gamma=0.5$	$\Gamma=1$	$\Gamma=0$	$\Gamma=0.5$	$\Gamma=1$
5	5.6505	5.7099	5.7682	2.3495	2.4326	2.4692
8	5.6505	5.7323	5.8224	2.3495	2.4556	2.5454
10	5.6505	5.7682	5.9123	2.3495	2.4692	2.6378

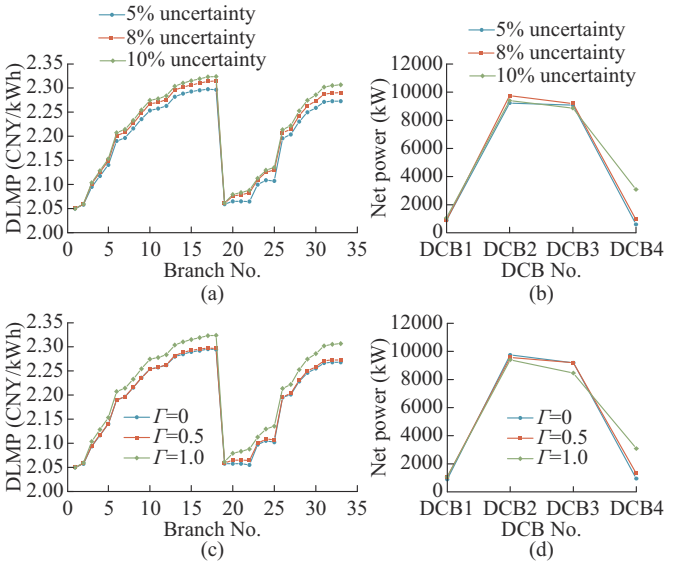

Fig. 15. Analysis of DLMPs and net power at time slot 18. (a) DLMPs with different uncertainties and $\Gamma=1$. (b) Net power with different uncertainties and $\Gamma=1$. (c) DLMPs with different Γ and 10% uncertainty. (d) Net power with different Γ and 10% uncertainty.

Under the same uncertainty, the increased value of the robustness control parameter Γ means the solution is more conservative, thus worsening the scenario with a higher cost. Taking 10% uncertainty at $t=18$ as an example, as shown in Fig. 15(c) and (d), the DLMPs also increase along with the parameter Γ as a whole due to a more conservative scenario with more IWs being dispatched to IDC4.

It is worth noting that if the level of uncertainty continues to increase, there may be no feasible solutions in the equilibrium optimization because some constraints of DSO may not be satisfied. For example, when uncertainty is 40% and $\Gamma=1$, the optimization is infeasible. Under this circumstance, the price-incentivized demand response of DCBs is not suitable for the system.

E. Computational Performance

The problem in the Subcase 3.2 consists of 21073 continuous variables and 864 binary variables. Massive binary variables might lead to computational difficulties. To demonstrate the scalability and computational performance of the proposed strategy, two additional test cases on the modified IEEE 69-bus system and 123-bus system are implemented. Detailed data can be found in [36]. In addition, the increasing number of DCBs also affects the number of binary variables. Another two cases with different numbers of DCBs in the modified IEEE 33-bus system presented in Section IV-A are compared in this subsection as well. The optimality gap tolerances are all set to be 1%.

The number of continuous and binary variables and the computational time with the proposed strategy are provided in Table VI. When applied to a larger-scale system, the computational time increases. However, the computation time also satisfies the computation demand for day-ahead scheduling. In practice, the distribution network is not very large in a data center park, and DCBs in adjacent locations can also be aggregated to a united DCB. This can reduce the number of binary variables and accelerate the computation process.

TABLE VI
SCALABILITY ANALYSIS OF PROPOSED EQUILIBRIUM OPTIMIZATION STRATEGY

System	Number of DCBs	Number of continuous variables	Number of binary variables	Time (s)
IEEE 33-bus	4	21073	864	3444.7
IEEE 69-bus	4	42673	864	12790.5
IEEE 123-bus	4	69673	864	14477.6
IEEE 33-bus	5	21481	1080	4905.7
IEEE 33-bus	6	26636	1296	6085.5

V. CONCLUSION

The paper develops a DLMP-based bi-level Stackelberg game framework between ISC and DSO in the DCP. At the upper level, ISC minimizes the electricity cost of all DCBs by dispatching IWs, BESS, SVG, and PV both temporally and spatially. The uncertainties of arriving IWs and PV generations for DCBs are considered and modeled using uncertainty sets. At the lower level, DSO minimizes the total electricity cost while satisfying the security-constrained operation of the distribution network. The model of proposed DLMP-based equilibrium optimization strategy is converted to a single-level MISOCP model using the strong duality theorem and binary expansion method.

A few numerical cases are studied on a modified IEEE 33-bus radial distribution network with four DCBs. Regarding DSO, the proposed strategy can stimulate the use of more flexible resources to support voltages and alleviate the distribution network congestion. Compared with centralized optimization, the DLMP-based equilibrium optimization strategy also reduces the cost of ISC by scheduling spatial and temporal demand-side resources with less exchanged information, which protects the privacy of the ISC. In addition, the proposed strategy can effectively accommodate the load-source uncertainties. Computational performance analysis has validated the scalability of the proposed strategy. The simulation results demonstrate that the proposed strategy offers a mutually beneficial solution for both DSO and ISC.

In future research, the cooperative game with an incentive-compatible mechanism among multiple ISCs in the distribution network will be an interesting topic.

APPENDIX A

Appendix A presents robust optimization. ξ^{front} and ξ^{PV}, which are the uncertainties of parameters $\tilde{L}_t^{\text{front}}$ and $\tilde{T}_t^{\text{PV}}$, are limited in the uncertainty set $\left[\left(1-\xi^{\text{front}}\right)L_t^{\text{front}},\left(1+\xi^{\text{front}}\right)L_t^{\text{front}}\right]$ and $\left[\left(1-\xi^{\text{PV}}\right)T_t^{\text{PV}},\left(1+\xi^{\text{PV}}\right)T_t^{\text{PV}}\right]$, respectively. According to the robust theorem presented in [29], the equivalent linear formulation of the robust problem in this paper can be modeled as:

$$\begin{cases} -\sum_{j\in D} L_{j,t}^{\text{DC}} + \Gamma_t^{\text{DC}} m_t^{\text{DC}} + n_t^{\text{DC}} \le -L_t^{\text{front}} \\ m_t^{\text{DC}} + n_t^{\text{DC}} \ge \xi^{\text{front}} L_t^{\text{front}} y_t^{\text{DC}} \\ m_t^{\text{DC}} \ge 0 \\ n_t^{\text{DC}} \ge 0 \\ y_t^{\text{DC}} \ge 1 \end{cases} \quad \forall t \in T \qquad \text{(A1)}$$

$$\begin{cases} P_{j,t}^{\text{PV}} + \Gamma_{j,t}^{\text{PV}} m_{j,t}^{\text{PV}} + n_{j,t}^{\text{PV}} \le S_{j,\max}^{\text{PV}} T_t^{\text{PV}} \\ m_{j,t}^{\text{PV}} + n_{j,t}^{\text{PV}} \ge \xi^{\text{PV}} T_t^{\text{PV}} y_{j,t}^{\text{PV}} \\ m_{j,t}^{\text{PV}} \ge 0 \\ n_{j,t}^{\text{PV}} \ge 0 \\ y_{j,t}^{\text{PV}} \ge 1 \end{cases} \quad \forall j \in D, \forall t \in T \qquad \text{(A2)}$$

where Γ_t^{DC} and $\Gamma_{j,t}^{\text{PV}}$ are to control the robustness against the uncertainty of $\tilde{L}_t^{\text{front}}$ and $\tilde{T}_t^{\text{PV}}$, respectively.

REFERENCES

[1] R. Danilak. (2017, Dec.). Why energy is a big and rapidly growing problem for data centers? [Online]. Available: https://www.forbes.com/sites/forbestechcouncil/2017/12/15/why-energy-is-a-big-and-rapidly-growing-problem-for-data-centers/?sh=3c06f8845a30
[2] E. Masanet, A. Shehabi, N. Lei *et al.*, "Recalibrating global data center energy-use estimates," *Science*, vol. 367, no. 6481, pp. 984-986, Feb. 2020.
[3] WikiLeaks. (2018, Oct.). Amazon Atlas. [Online]. Available: https://wikileaks.org/amazon-atlas/
[4] Starhub. (2022, Jul.). A trusted and reliable data center partner to meet your

businesses' evolving demands. [Online]. Available: https://www.starhub.com/business/products-and-services/hosting-my-business/data-centre.html

[5] Z. Liu, H. Yu, R. Liu *et al.*, "Configuration optimization model for data-center-park-integrated energy systems under economic, reliability, and environmental considerations," *Energies*, vol. 13, no. 2, p. 448, Jan. 2020.

[6] J. Zhao, A. Arefi, A. Borghetti *et al.*, "Indices of congested areas and contributions of customers to congestions in radial distribution networks," *Journal of Modern Power Systems and Clean Energy*, vol. 10, no. 3, pp. 656-666, May 2022.

[7] N. C. Koutsoukis, D. O. Siagkas, P. S. Georgilakis *et al.*, "Online reconfiguration of active distribution networks for maximum integration of distributed generation," *IEEE Transactions on Automation Science and Engineering*, vol. 14, no. 2, pp. 437-448, Apr. 2017.

[8] L. Bai, J. Wang, C. Wang *et al.*, "Distribution locational marginal pricing (DLMP) for congestion management and voltage support," *IEEE Transactions on Power Systems*, vol. 33, no. 4, pp. 4061-4073, Jul. 2018.

[9] X. Yan, C. Gu, X. Zhang *et al.*, "Robust optimization-based energy storage operation for system congestion management," *IEEE Systems Journal*, vol. 14, no. 2, pp. 2694-2702, Jun. 2020.

[10] B. S. K. Patnam and N. M. Pindoriya, "DLMP calculation and congestion minimization with EV aggregator loading in a distribution network using bilevel program," *IEEE Systems Journal*, vol. 15, no. 2, pp. 1835-1846, Jun. 2021.

[11] Z. Zhao, Y. Liu, L. Guo *et al*., "Locational marginal pricing mechanism for uncertainty management based on improved multi-ellipsoidal uncertainty set," *Journal of Modern Power Systems and Clean Energy*, vol. 9, no. 4, pp. 734-750, Jul. 2021.

[12] X. Yan, C. Gu, F. Li *et al.*, "LMP-based pricing for energy storage in local market to facilitate PV penetration," *IEEE Transactions on Power Systems*, vol. 33, no. 3, pp. 3373-3382, May 2018.

[13] M. Chen, C. Gao, M. Song *et al.*, "Internet data centers participating in demand response: a comprehensive review," *Renewable and Sustainable Energy Reviews*, vol. 117, p. 109466, Jan. 2020.

[14] Q. Sun, C. Wu, Z. Li *et al.*, "Colocation demand response: joint online mechanisms for individual utility and social welfare maximization," *IEEE Journal on Selected Areas in Communications*, vol. 34, no. 12, pp. 3978-3992, Dec. 2016.

[15] China Daily. (2022, Mar.). Western regions to gain computing power. [Online]. Available: https://global.chinadaily.com.cn/a/202203/17/WS62329784a310fd2b29e51734.html

[16] C. Jiang, C. Tseng, Y. Wang *et al.*, "Optimal pricing strategy for data center considering demand response and renewable energy source accommodation," *Journal of Modern Power Systems and Clean Energy*, vol. 11, no. 1, pp. 345-354, Jan. 2023.

[17] H. Wang, J. Huang, X. Lin *et al.*, "Proactive demand response for data centers: a win-win solution," *IEEE Transactions on Smart Grid*, vol. 7, no. 3, pp. 1584-1596, May 2016.

[18] Z. Yang, M. Ni, and H. Liu, "Pricing strategy of multi-energy provider considering integrated demand response," *IEEE Access*, vol. 8, pp. 149041-149051, Aug. 2020.

[19] J. Zhang, X. Huang, and R. Yu, "Optimal task assignment with delay constraint for parked vehicle assisted edge computing: a Stackelberg game approach," *IEEE Communications Letters*, vol. 24, no. 3, pp. 598-602, Mar. 2020.

[20] X. Wu and A. J. Conejo, "Distribution market including prosumers: an equilibrium analysis," *IEEE Transactions on Smart Grid*, vol. 14, no. 2, pp. 1495-1504, Feb. 2022.

[21] H. Sekhavatmanesh and R. Cherkaoui, "A novel decomposition solution approach for the restoration problem in distribution networks," *IEEE Transactions on Power Systems*, vol. 35, no. 5, pp. 3810-3824, Sept. 2020.

[22] S. Fattaheian-Dehkordi, M. Tavakkoli, A. Abbaspour *et al.*, "An incentive-based mechanism to alleviate active power congestion in a multi-agent distribution system," *IEEE Transactions on Smart Grid*, vol. 12, no. 3, pp. 1978-1988, May 2021.

[23] Z. Chen, L. Wu, and Z. Li, "Electric demand response management for distributed large-scale internet data centers," *IEEE Transactions on Smart Grid*, vol. 5, no. 2, pp. 651-661, Mar. 2014.

[24] Z. Ding, L. Xie, Y. Lu *et al.*, "Emission-aware stochastic resource planning scheme for data center microgrid considering batch workload scheduling and risk management," *IEEE Transactions on Industry Applications*, vol. 54, no. 6, pp. 5599-5608, Nov.-Dec. 2018.

[25] X. Yan, C. Gu, X. Zhang *et al.*, "Robust optimization-based energy storage operation for system congestion management," *IEEE Systems Journal*, vol. 14, no. 2, pp. 2694-2702, Jun. 2020.

[26] T. Chen, Y. Zhang, X. Wang *et al.*, "Robust workload and energy management for sustainable data centers," *IEEE Journal on Selected Areas in Communications*, vol. 34, no. 3, pp. 651-664, Mar. 2016.

[27] C. Duan, W. Fang, L. Jiang *et al.*, "Distributionally robust chance-constrained approximate AC-OPF with Wasserstein metric," *IEEE Transactions on Power Systems*, vol. 33, no. 5, pp. 4924-4936, Sept. 2018.

[28] Z. Yuan, P. Li, Z. Li *et al.*, "Data-driven risk-adjusted robust energy management for microgrids integrating demand response aggregator and renewable energies," *IEEE Transactions on Smart Grid*, vol. 14, no. 1, pp. 365-377, Jan. 2023.

[29] D. Bertsimas and M. Sim, "The price of robustness," *Operations Research*, vol. 52, no. 1, pp. 35-53, Feb. 2004.

[30] J. Wei, Y. Zhang, J. Wang *et al.*, "Distribution LMP-based demand management in industrial park via a bi-level programming approach," *IEEE Transactions on Sustainable Energy*, vol. 12, no. 3, pp. 1695-1706, Jul. 2021.

[31] J. Wan, X. Gui, R. Zhang *et al.*, "Joint cooling and server control in data centers: a cross-layer framework for holistic energy minimization," *IEEE Systems Journal*, vol. 12, no. 3, pp. 2461-2472, Sept. 2018.

[32] T. Xu, T. Ding, O. Han *et al.*, "Counterpart and correction for strong duality of second-order conic program in radial networks," *IEEE Transactions on Power Systems*, vol. 37, no. 5, pp. 4117-4120, Sept. 2022.

[33] W. Liu, S. Chen, Y. Hou *et al.*, "Optimal reserve management of electric vehicle aggregator: discrete bilevel optimization model and exact algorithm," *IEEE Transactions on Smart Grid*, vol. 12, no. 5, pp. 4003-4015, Sept. 2021.

[34] G. Chen, H. Zhang, H. Hui *et al.*, "Scheduling thermostatically controlled loads to provide regulation capacity based on a learning-based optimal power flow model," *IEEE Transactions on Sustainable Energy*, vol. 12, no. 4, pp. 2459-2470, Oct. 2021.

[35] Shanghai Municipal People's Government. (2020, Dec.). Notice of Shanghai Municipal Development and Reform Commission on reducing electricity prices for large industries in Shanghai. [Online]. Available: https://www.shanghai.gov.cn/nw49248/20201204/82b0c749089345e1aa55f68672b9ebbd.html

[36] Z. Yang. (2022, May). Optimal DLMP-based equilibrium dispatching strategy of spatial-temporal demand-side resources in data center park. [Online]. Available: https://dx.doi.org/10.21227/axfq-bq57

Zhihao Yang received the B.S. degree in electrical engineering and automation from Jiangsu University of Science and Technology, Zhangjiagang, China, in 2016, and the M.S. degree in power systems and automation from Hohai University, Nanjing, China, in 2019. He is currently pursuing the Ph.D. degree in electrical engineering at Hohai University. His research interests include distribution network operation and demand response.

Anupam Trivedi received a dual degree (integrated bachelor's and master's) in civil engineering from the Indian Institute of Technology Bombay, Mumbai, India, in 2009, and the Ph.D. degree from National University of Singapore, Singapore, in 2015. He is currently a Senior Research Fellow at the Department of Electrical & Computer Engineering, National University of Singapore. His research interests include evolutionary algorithms, multi-objective optimization, constrained optimization, and smart grid optimization.

Ming Ni received the B.S. and Ph.D. degrees from Southeast University, Nanjing, China, in 1991 and 1996, respectively. He is an Adjunct Ph.D. Supervisor with the College of Energy and Electrical Engineering, Hohai University, Nanjing, China. His research interests include power system planning, analysis and control, and cyber-physical systems.

Haoming Liu received the B.S., M.S., and Ph.D. degrees from Nanjing University of Science and Technology, Nanjing, China, in 1998, 2001, and 2003, respectively. He is currently a Professor at the College of Energy and Electrical Engineering, Hohai University, Nanjing, China. His research interests include renewable energy generation, distribution system analysis and control, and the electricity market.

Dipti Srinivasan received the M.S. and Ph.D. degrees from National University of Singapore, Singapore, in 1991 and 1994, respectively. She is currently a Professor at the Department of Electrical & Computer Engineering, National University of Singapore. Her main research interests include optimization and control, wind and solar power prediction, electricity price prediction, deep learning, and development of multi-agent systems for system operation and control.